Article

Not peer-reviewed version

Robust Intrinsic Dorsoventral Organization of Hippocampal Sharp Wave–Ripples Persists During Cannabinoid Modulation

Athina Miliou , Penny Giannakopoulou , Agathi Erda , Alexia-Ioanna Tsiokou , Eleni-Despoina Mavriki , Giota Tsotsokou , Ioanna-Maria Sotiropoulou , Costas Papatheodoropoulos *

Posted Date: 15 April 2026

doi: 10.20944/preprints202604.1018.v1

Keywords: hippocampus; dorsoventral; neuromodulation; endocannabinoids; cannabidiol; sharp wave–ripples; brain rhythms

 doi:10.20944/preprints202604.1018.v1

Article

Robust Intrinsic Dorsoventral Organization of Hippocampal Sharp Wave–Ripples Persists During Cannabinoid Modulation

Athina Miliou [1], Penny Giannakopoulou [1], Agathi Erda [1], Alexia-Ioanna Tsiokou [1], Eleni-Despoina Mavriki [1], Giota Tsotsokou [1], Ioanna-Maria Sotiropoulou [1] and Costas Papatheodoropoulos [2,*]

[1] Lab of Physiology, Department of Medicine, University of Patras, Greece; athinamiliou@ac.upatras.gr

[2] Lab of Experimental Animals, School of Health Sciences, and Lab of Physiology, Department of Medicine, University of Patras, Greece

* Correspondence: cepapath@upatras.gr

Abstract

Background/Objectives: The hippocampus exhibits marked functional heterogeneity along its dorsoventral axis, with dorsal regions primarily supporting cognitive and spatial processing and ventral regions linked to emotional and stress-related functions. This functional gradient is shaped by intrinsic circuit properties and neuromodulatory systems, including the endocannabinoid system, whose cannabinoid type 1 (CB_1) receptors are abundantly expressed in the hippocampus. Sharp wave–ripple (SWR) complexes are highly organized network events that depend on precise excitation/inhibition balance and are essential for hippocampal information processing. The present study aimed to determine whether cannabinoid receptor activation or modulation influences SWRs and associated neuronal activity along the dorsoventral axis of the hippocampus. **Methods**: Extracellular field potentials and multiunit activity were recorded from the stratum pyramidale of the CA1 region in acute hippocampal slices obtained from dorsal and ventral segments. Spontaneous SWRs were analyzed under control conditions and following application of the CB_1 receptor agonists ACEA and WIN55,212-2, the cannabinoid compound cannabidiol (CBD), and the GIRK channel blocker tertiapin-Q. SWR incidence, waveform characteristics, and multiunit activity were quantified and compared between hippocampal segments. CB1 receptor expression was assessed in dorsal and ventral CA3 using Western blot analysis. **Results**: Baseline recordings revealed pronounced dorsoventral differences in SWR dynamics, with ventral hippocampus exhibiting higher SWR rates, larger amplitudes, and enhanced neuronal recruitment compared to dorsal hippocampus. In contrast, activation of CB_1 receptors by ACEA and WIN55,212-2, as well as application of CBD, did not significantly alter SWR occurrence, waveform properties, or associated multiunit activity in either hippocampal segment. Similarly, blockade of GIRK channels produced only limited effects, restricted to modulation of ripple power, and did not reveal a latent sensitivity of SWRs to cannabinoid receptor activation. Notably, CB1 receptor expression in the CA3 region was comparable between dorsal and ventral hippocampus. **Conclusions**: These findings demonstrate that spontaneous SWRs in hippocampal slices are robust to acute cannabinoid modulation despite strong CB_1 receptor expression. The intrinsic dorsoventral organization of hippocampal network dynamics persists under cannabinoid receptor activation, indicating that SWR generation is primarily based on local circuit properties rather than fast endocannabinoid signaling. This resistance has important implications for understanding how cannabinoids influence hippocampal function in vivo, suggesting that their cognitive and behavioral effects are likely mediated through modulation of large-scale network interactions rather than direct disruption of intrinsic SWR-generating mechanisms.

Keywords: hippocampus; dorsoventral; neuromodulation; endocannabinoids; cannabidiol; sharp wave—ripples; brain rhythms

 doi:10.20944/preprints202604.1018.v1

1. Introduction

Sharp wave–ripples (SWRs) are transient hippocampal population events characterized by a large sharp wave in the local field potential (LFP) accompanied by fast ripple oscillations (140–250 Hz), and represent one of the most synchronous patterns in the mammalian brain [1]. They occur predominantly during quiet wakefulness and non-REM sleep and are tightly linked to the reactivation of hippocampal neuronal ensembles, thereby supporting memory consolidation and hippocampal-cortical communication [1–3]. The generation of SWRs depends on precisely coordinated interactions between excitatory inputs, primarily arising from CA3, and local inhibitory interneuron networks in CA1. Consequently, even subtle shifts in excitation/inhibition (E/I) balance can profoundly alter SWR occurrence and structure, making these events a sensitive index of hippocampal network dynamics and neuromodulatory influences.

The endocannabinoid system constitutes a major neuromodulatory framework regulating synaptic transmission, neuronal excitability, and behavior, including cognition, learning, memory, and emotional processing [4,5]. Endocannabinoids act primarily through cannabinoid type 1 (CB1) receptors, which are abundantly expressed in the hippocampus, predominantly on presynaptic terminals of GABAergic interneurons, particularly cholecystokinin-positive basket cells, and, to a lesser extent, on glutamatergic terminals [6,7]. CB1 receptors couple mainly to Gi/o proteins and modulate multiple intracellular pathways, including inhibition of adenylate cyclase, suppression of voltage-gated Ca^{2+} channels, and regulation of G-protein-gated inwardly rectifying K^+ (GIRK) channels. Through these mechanisms, CB1 receptor activation reduces neurotransmitter release and dynamically regulates the E/I balance of hippocampal circuits [8,9]. Classical forms of endocannabinoid signaling, such as depolarization-induced suppression of inhibition or excitation, exemplify this activity-dependent retrograde control of synaptic transmission [10,11].

Pharmacological activation of CB1 receptors has been reported to alter hippocampal network oscillations associated with cognitive function. In vivo studies have shown that cannabinoids such as Δ^9-tetrahydrocannabinol (THC) and CP55,940 reduce theta and gamma oscillations and impair hippocampus-dependent behavior [12]. In vitro studies further indicate that CB1 receptor activation can modulate intrinsic hippocampal rhythms, including gamma oscillations and SWRs, likely through presynaptic inhibition of excitatory transmission and altered interneuron–pyramidal coordination [13–15]. However, the magnitude and consistency of these effects vary across experimental conditions, and their dependence on circuit context and analytical approach remains incompletely understood.

In contrast to CB1 receptor agonists, cannabidiol (CBD) is a non-intoxicating phytocannabinoid with a more complex and indirect mode of action. CBD exhibits low affinity for the orthosteric CB1 receptor site but can act as a negative allosteric modulator, reducing the efficacy and potency of CB1 receptor agonists [16,17]. In addition, CBD interacts with multiple molecular targets, including 5-HT_1A, TRPV, and GPR55 receptors, thereby exerting context-dependent effects on neuronal excitability [18]. Despite its increasing clinical relevance, relatively little is known about how CBD influences hippocampal network oscillations, and in particular whether it modulates SWRs directly or alters their properties through interactions with CB1-dependent mechanisms.

An additional and critical dimension in understanding cannabinoid effects on hippocampal function is the pronounced functional and anatomical heterogeneity along the dorsoventral (septotemporal) axis of the hippocampus. The dorsal hippocampus is primarily involved in spatial learning and memory, whereas the ventral hippocampus contributes more strongly to emotional and stress-related processes [19–21]. These functional differences are paralleled by distinct connectivity patterns, intrinsic excitability, synaptic organization, and E/I balance along the longitudinal axis [22]. Such regional specialization gives rise to segment-specific network dynamics, including differences in oscillatory activity and short-term neuronal responses. Importantly, SWRs themselves exhibit dorsoventral heterogeneity. Both in vivo and in vitro studies have reported differences in SWR

 doi:10.20944/preprints202604.1018.v1

incidence, waveform characteristics, and susceptibility to perturbations along the hippocampal axis [23–26]. These observations suggest that neuromodulatory systems, including the endocannabinoid system, may exert region-specific effects on SWR-generating circuits. Nevertheless, most previous studies examining cannabinoid effects on hippocampal oscillations have focused on a single hippocampal segment and have not systematically addressed dorsoventral differences.

Taken together, these considerations raise key unresolved questions: whether cannabinoid signaling modulates SWR activity in a segment-specific manner along the hippocampal axis, and whether different classes of cannabinoids, such as CB1 receptor agonists and CBD, exert distinct effects on SWR dynamics depending on regional circuit properties. Addressing these questions is essential for linking cellular and network-level cannabinoid actions to their differential impact on cognitive and emotional processes.

In the present study, we investigated the effects of cannabinoid signaling on SWR activity along the dorsoventral axis of the hippocampus. Using extracellular recordings from the CA1 region in dorsal and ventral hippocampal slices, we examined how CB1 receptor agonists and CBD influence SWR occurrence, waveform properties, and associated neuronal activity. Our aim was to determine whether cannabinoid modulation of hippocampal network dynamics is region-specific and to elucidate how intrinsic circuit organization interacts with cannabinoid signaling to shape SWR activity.

2. Materials and Methods

2.1. Experimental Animals and Hippocampal Slice Preparation

Male Wistar rats were obtained from the Animal Facility of the Medical School of the University of Patras (license No: EL-13-BIOexp-04) and housed under controlled environmental conditions (21 ± 1 °C; 12 h light/dark cycle) with ad libitum access to food and water. All procedures were conducted in accordance with the European Directive 2010/63/EU. The animal study protocol was approved by the Research Ethics Committee of the University of Patras and the Directorate of Veterinary Services of the Achaia Prefecture of Western Greece Region (reg. number: 5661/37, 18 January 2021). The number of animals used was determined based on power analysis (G*Power software). Animals were deeply anesthetized and decapitated, and the brains were rapidly removed and immersed in ice-cold (~4 °C) artificial cerebrospinal fluid (ACSF) containing (in mM): 124 NaCl, 4 KCl, 2 $CaCl_2$, 2 $MgSO_4$, 26 $NaHCO_3$, 1.25 NaH_2PO_4, and 10 glucose (pH 7.4).

The hippocampi were dissected, and 500 μm-thick transverse slices were prepared from both dorsal and ventral regions using a McIlwain tissue chopper, following established procedures. Slices were transferred to an interface-type recording chamber and continuously perfused with ACSF equilibrated with 95% O_2 and 5% CO_2 at a flow rate of ~1.5 ml/min. The temperature was maintained at 30 ± 0.5 °C, and the chamber atmosphere was humidified with the same gas mixture. Recordings were initiated after a recovery period of at least 90 minutes.

2.2. Electrophysiology and Data Analysis

Spontaneous field potentials were recorded from the CA1 region of hippocampal slices, with electrodes positioned in the stratum pyramidale to monitor population activity and, in selected experiments, in the stratum radiatum or CA3 pyramidal layer to assess network interactions. Recordings were obtained using carbon fiber electrodes under visual guidance and amplified, band-pass filtered (0.5 Hz–2 kHz), and digitized at 10 kHz for offline analysis. Spontaneous activity consisted of sharp wave–ripple complexes (SWRs) and multiunit activity (MUA). SWRs were identified in the CA1 pyramidal layer as large-amplitude events with superimposed high-frequency oscillations. Events occurred either in isolation or in clusters, defined as sequences of SWRs separated by short inter-event intervals (intra-cluster interval, ~100 ms), identified from inter-event interval (IEI) distributions. For SWR analysis, signals were down-sampled to 1 kHz and low-pass filtered at 35 Hz to isolate the sharp wave component. Events were detected using threshold-based procedures

 doi:10.20944/preprints202604.1018.v1

followed by visual verification. The following parameters were quantified: (i) SWR amplitude; (ii) inter-event interval (IEI); (iii) probability of cluster occurrence; (iv) ripple peak frequency; (v) ripple power. Ripple frequency and power were quantified following spectral analysis of local field potentials performed using Fast Fourier Transform (FFT). Power spectra were computed from continuous recordings using a Hanning window with a duration of 1.638 s, yielding a frequency resolution of approximately 0.61 Hz. Ripple peak frequency was defined as the frequency corresponding to the maximum power within the band between 75 and 250 Hz. Ripple power was quantified as the peak value of the power spectrum within the ripple range.

MUA was extracted from band-pass filtered signals (400 Hz–1.5 kHz) and detected using threshold-based spike identification with visual confirmation. MUA occurring between SWRs was defined as MUA-Base, while MUA occurring during SWRs was defined as MUA-SWR. MUA-Base was quantified as firing rate (spikes/s) during inter-SWR periods, whereas MUA-SWR was quantified as the peak firing rate derived from peri-event time histograms aligned to SWR peaks. The temporal relationship between unit firing and SWR peak was quantified as MUA-Delay. For each slice, SWR and MUA parameters were quantified during control conditions, after drug application, and after washing out the drug, using stable recording periods (5 last minutes of each period). Drug effects were expressed as within-slice changes relative to control.

The following drugs were used in this study: the potent and highly selective agonist of CB1 receptors N-(2-Chloroethyl)-5Z,8Z,11Z,14Z-eicosatetraenamide (ACEA), the potent aminoalkylindole cannabinoid receptor agonist [(3R)-2,3-dihydro-5-methyl-3-(4-morpholinylmethyl)pyrrolo [1,2,3-de]-1,4-benzoxazin-6-yl]-1-naphthalenyl-methanone, monomethane sulfonate ((+)-WIN 55,212-2 (mesylate)), and the natural cannabinoid Cannabidiol (2-[(1R,6R)-3-Methyl-6-(1-methylethenyl)-2-cyclohexen-1-yl]-5-pentyl-1,3-benzenediol, CBD), and Tertiapin Q (trifluoroacetate salt, TPN-Q). ACEA and CBD were purchased from Tocris Cookson Ltd., UK, WIN 55,212-2 and Tertiapin-Q was purchased from Cayman Chemical Company, USA. Also, CBD was kindly provided by Dr. Maria Chalampalaki (Faculty of Pharmacy, National and Kapodistrian University of Athens, Greece).

2.3. Immunoblotting

To assess CB1 receptor expression along the dorsoventral axis, the CA3 region was isolated from dorsal and ventral hippocampal slices and homogenized in 1% SDS containing protease inhibitors. Protein concentration was determined spectrophotometrically. Equal amounts of protein (25 μg per lane) were separated by SDS-PAGE and transferred onto PVDF membranes. Membranes were blocked in 5% non-fat milk in PBST and incubated overnight at 4 °C with primary antibodies against CB1 (rabbit monoclonal, 1:1000, Abcam) and β-actin (mouse monoclonal, 1:10000, Thermo Fisher Scientific). After washing, membranes were incubated with appropriate HRP-conjugated secondary antibodies. Protein bands were visualized using enhanced chemiluminescence and imaged with a ChemiDoc MP system (Bio-Rad). Band intensities were quantified using ImageLab software, and CB1 expression was normalized to β-actin. Data are expressed as the ratio of CB1 to β-actin optical density for each sample.

2.4. Statistics

The experimental unit in this study was the hippocampal slice. Each slice was exposed to a single pharmacological condition, and comparisons were performed between control and drug application within the same slice. Data were analyzed using linear mixed-effects models (LMMs) to account for repeated measurements within slices. For each dependent variable (SWR and MUA parameters), fixed effects included Drug condition (control vs drug), Hippocampal region (dorsal vs ventral), and their interaction. A random intercept was included for slice to account for within-slice dependencies. The primary effect of interest was the interaction between Drug and Region (dorsal—ventral), indicating differential drug effects along the dorsoventral axis. When appropriate, post hoc comparisons were performed using estimated marginal means with correction for multiple

 doi:10.20944/preprints202604.1018.v1

comparisons. Given the limited number of slices per animal, animal identity was not included as a random factor, in line with standard practice in slice electrophysiology studies. Model assumptions were assessed by visual inspection of residuals. When necessary, data were log-transformed to improve normality and homoscedasticity. For descriptive purposes, within-slice changes (Δ or percentage change from control) were also calculated. Diamond plots display the median, interquartile range (25th–75th percentiles), mean, 5th and 95th percentiles, and outliers. Comparisons between the dorsal and ventral hippocampus across the measured variables were conducted using an independent-samples t-test. Statistical significance was set at $p < 0.05$.

3. Results

3.1. Baseline Characteristics of Sharp Wave-Ripples Along the Dorsoventral Hippocampal Axis

Spontaneous network activity in the CA1 region was characterized by recurrent SWRs recorded from the stratum pyramidale, as well as multiunit activity (MUA) occurring either during SWR events or independently (Figure 1A,B). Under control conditions, SWR complexes occurred intermittently and were readily detected in both dorsal and ventral hippocampal slices (Figure 1A). Quantitative analysis, however, revealed pronounced differences in several SWR properties along the dorsoventral axis. The inter-event interval (IEI) was significantly shorter in ventral compared with dorsal hippocampus (independent samples t-test, $p < 0.001$), indicating a higher rate of spontaneous SWR generation in ventral CA1 (Figure 1D). In contrast, the probability of SWR clustering did not differ significantly between regions ($p = 0.987$), suggesting similar temporal grouping of events despite differences in overall occurrence rate. Analysis of SWR waveform properties showed that sharp wave amplitude was significantly greater in ventral slices ($p < 0.001$). In addition, both ripple frequency and ripple power were higher in ventral compared to dorsal hippocampus ($p = 0.045$ and $p = 0.034$, respectively), indicating differences in the fast oscillatory component of SWRs along the dorsoventral axis.

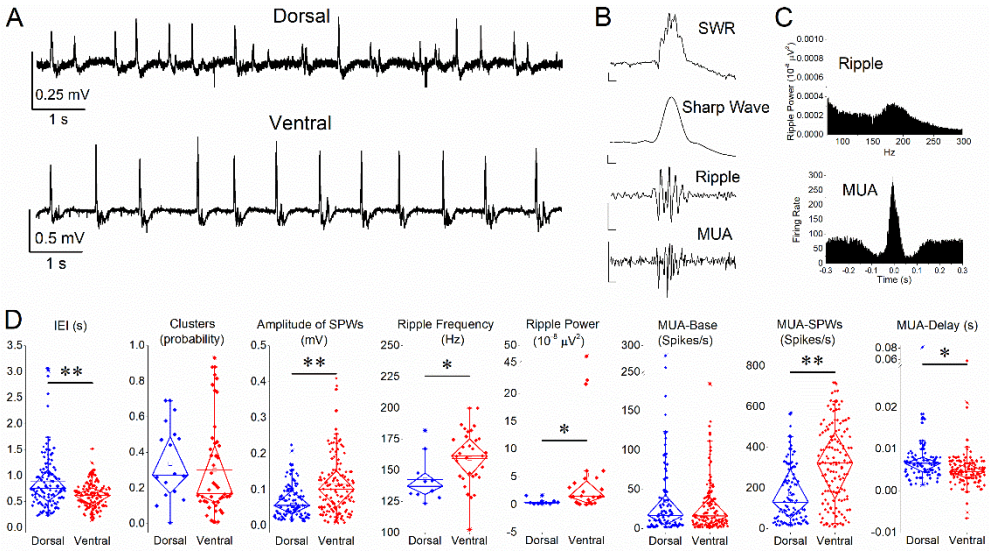

Figure 1. Baseline properties of SWRs and associated neuronal activity in dorsal and ventral hippocampus. (**A**) Representative extracellular field recordings from the CA1 stratum pyramidale illustrating spontaneous SWRs in dorsal (top) and ventral (bottom) hippocampal slices under control conditions. (**B**) Example of an individual SWR event. Top trace: raw signal (SWR). Middle traces: low-pass filtered signal (35 Hz) showing the sharp wave component and band-pass filtered signal (90–250 Hz) showing ripple oscillations. Bottom trace: band-pass filtered signal ()0.4—1.5 kHz) revealing multiunit activity (MUA). Calibration bars: 50 μV, 10 ms. (**C**) Representative spectral and temporal characteristics of SWRs. Top: ripple power spectrum. Bottom: peri-event time histogram of MUA aligned to the SWR peak. (**D**) Quantification of SWR and MUA parameters in dorsal (blue) and ventral (red) hippocampus, including inter-event interval (IEI), probability of clustered events, sharp

 doi:10.20944/preprints202604.1018.v1

wave amplitude, ripple frequency, ripple power, baseline firing rate (MUA-Base), SWR-associated firing rate (MUA-SWR), and MUA delay relative to SWR peak (MUA-Delay). Significant differences between dorsal and ventral hippocampus are indicated (independent t-test, *$p < 0.05$, **$p < 0.01$).

Baseline neuronal firing was assessed using MUA (Figure 1B,D). MUA recorded outside SWRs (MUA-Base) did not differ between dorsal and ventral hippocampus ($p = 0.971$), indicating comparable baseline excitability. In contrast, MUA associated with SWRs (MUA-SWR) was significantly higher in ventral slices ($p < 0.001$), reflecting enhanced neuronal recruitment during SWR events. Furthermore, the timing of neuronal firing relative to the SWR peak (MUA-Delay) differed significantly between regions ($p = 0.038$), indicating altered temporal coordination of unit activity within SWRs along the dorsoventral axis.

Taken together, these results demonstrate that SWRs in the ventral hippocampus occur more frequently, exhibit larger amplitudes and stronger ripple components, and recruit more robust and temporally distinct neuronal firing compared to dorsal hippocampus, while baseline firing rates remain comparable between regions.

These findings are broadly consistent with previous in vitro studies reporting enhanced SWR activity and neuronal recruitment in ventral hippocampus [23,26–28]. However, in contrast to in vivo studies reporting larger SPW amplitudes in dorsal hippocampus [29,30], the present data show greater amplitudes in ventral slices. This discrepancy likely reflects methodological differences, as in vivo recordings preserve extrahippocampal inputs and longitudinal hippocampal connectivity, whereas transverse slice preparations isolate local circuitry [31,32]. Accordingly, slice recordings primarily reflect intrinsic dorsoventral differences in local network dynamics, whereas in vivo measurements capture the integrated activity of the longitudinal hippocampal system [29,33].

3.2. Effects of ACEA on SWRs and Neuronal Activity

To investigate the role of CB1 receptor activation in the regulation of hippocampal network oscillations, slices were exposed to the selective CB1 agonist ACEA. Activation of CB1 receptors with ACEA did not significantly affect any of the examined properties of spontaneous SWRs or associated neuronal activity. Linear mixed-model analysis revealed no effect of condition on inter-event interval (IEI), cluster probability, sharp wave amplitude, ripple frequency, or ripple power (all $p > 0.5$) (Figures 2 and 3). Similarly, ACEA did not alter baseline multiunit activity (MUA-Base), SWR-associated firing (MUA-SWR), or the temporal delay of neuronal firing relative to SWR peaks (MUA-Delay) (all $p > 0.2$). No significant condition × region interactions were observed for any parameter (all $p > 0.7$), indicating that CB1 receptor activation did not differentially affect dorsal and ventral hippocampal slices. In contrast, significant main effects of hippocampal segment were consistently observed for several variables, including IEI, SWR amplitude, and MUA measures (all $p < 0.05$), confirming robust dorsoventral differences in baseline network activity.

3.3. Effects of WIN 55,212-2 on SWRs and Neuronal Activity

Application of WIN 55,212-2 did not significantly alter SWR properties or neuronal firing (Figures 4 and 5). No significant effects of condition were observed on IEI, cluster probability, amplitude, MUA-Base, MUA-SWR, or MUA-Delay (all $p > 0.5$), and no condition × region interactions were detected (all $p > 0.4$). Significant main effects of hippocampal segment persisted for several parameters, including IEI, amplitude, and MUA-SWR (all $p < 0.05$), indicating that dorsoventral differences in network dynamics remained unaffected by WIN. Due to incomplete observations in some condition × region combinations, ripple frequency and ripple power were not suitable for full factorial evaluation in this dataset.

 doi:10.20944/preprints202604.1018.v1

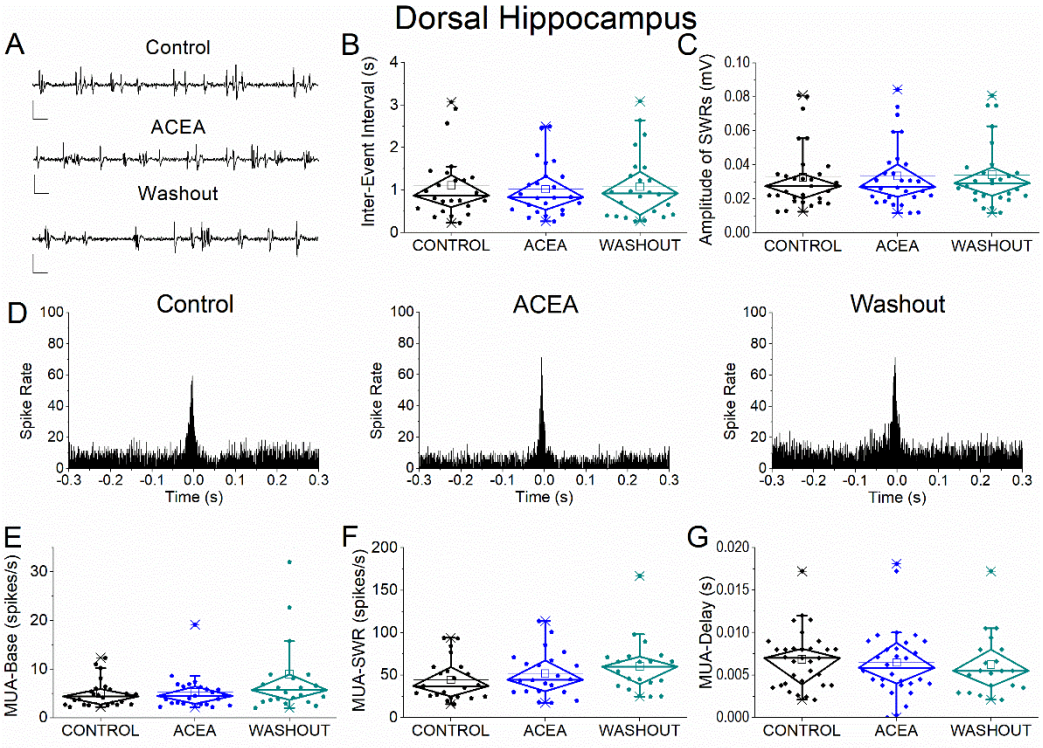

Figure 2. Effects of the CB1 receptor agonist ACEA on SWRs and MUA in dorsal hippocampus. (**A**) Representative extracellular recordings from CA1 stratum pyramidale under control conditions (top), during ACEA application (middle), and after washout (bottom). Calibration bars: 50 μV, 0.5 s. (**B–C**) Quantification of SWR properties across conditions. (**B**) Inter-event interval (IEI). (**C**) Sharp wave amplitude. No significant effects of ACEA were observed. (**D**) Peri-event time histograms of MUA aligned to SWR peak under control (left), ACEA (middle), and washout (right) conditions. (**E–G**) Quantification of neuronal activity parameters. (**E**) Baseline firing rate (MUA-Base). (**F**) SWR-associated firing rate (MUA-SWR). (**G**) MUA delay relative to SWR peak (MUA-Delay). No significant effects of ACEA were detected for any parameter. Statistical analysis was performed using LMM (Control vs ACEA).

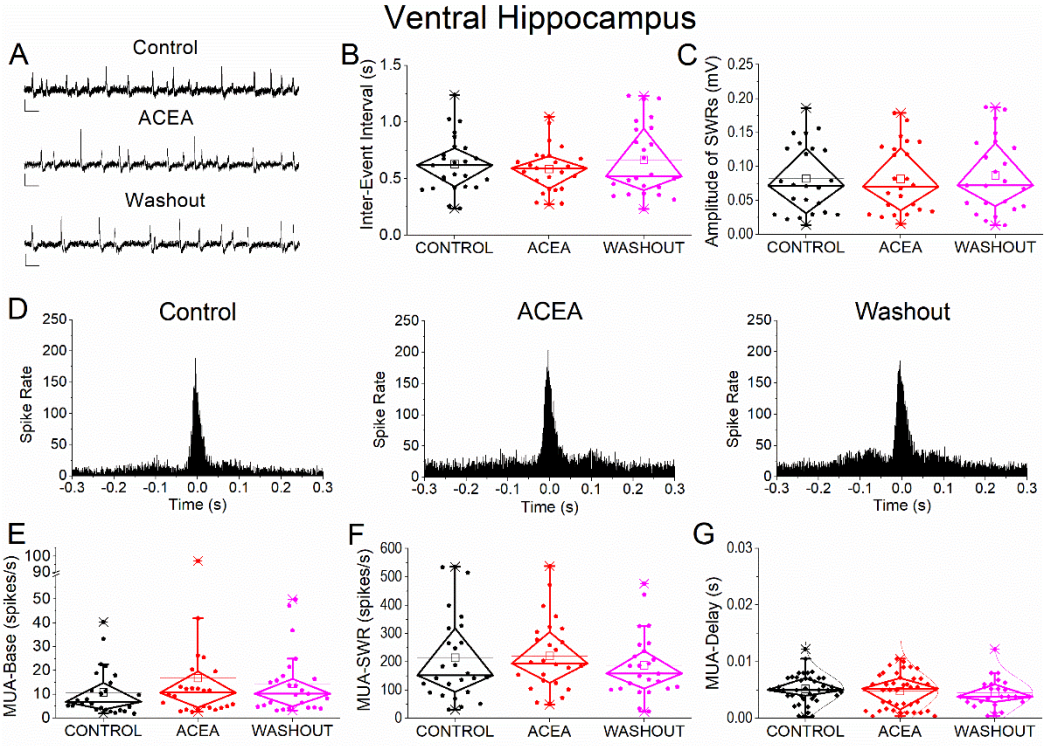

 doi:10.20944/preprints202604.1018.v1

Figure 3. Effects of the CB1 receptor agonist ACEA on SWRs and MUA in ventral hippocampus. (**A**) Representative extracellular recordings from CA1 stratum pyramidale under control conditions (top), during ACEA application (middle), and after washout (bottom). Calibration bars: 50 μV, 0.5 s. (**B–C**) Quantification of SWR properties across conditions. (**B**) Inter-event interval (IEI). (**C**) Sharp wave amplitude. No significant effects of ACEA were observed. (**D**) Peri-event time histograms of multiunit activity (MUA) aligned to SWR peak under control (left), ACEA (middle), and washout (right) conditions. (**E–G**) Quantification of MUA. (**E**) Baseline firing rate (MUA-Base). (**F**) SWR-associated firing rate (MUA-SWR). (**G**) MUA delay relative to SWR peak (MUA-Delay). No significant effects of ACEA were detected for any parameter. Statistical analysis was performed using LMM (Control vs ACEA). Washout data are shown for completeness but were not included in statistical comparisons.

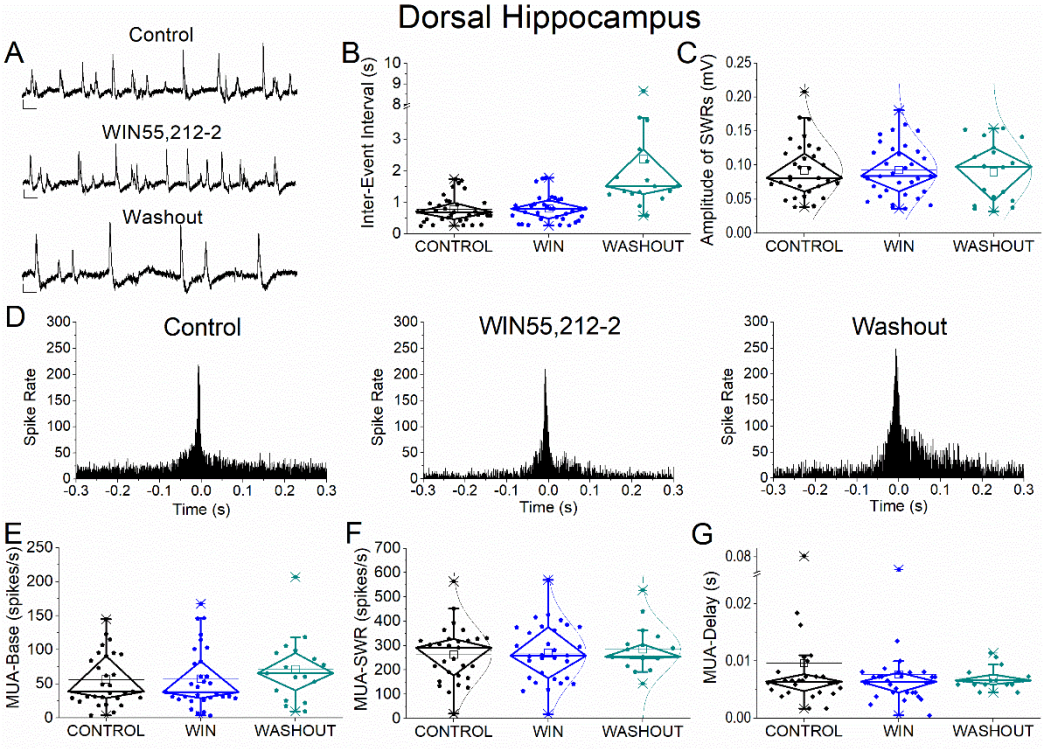

Figure 4. Effects of the cannabinoid receptor agonist WIN55,212-2 on SWRs and MUA in dorsal hippocampus. (**A**) Representative extracellular recordings from CA1 stratum pyramidale under control conditions (top), during WIN55,212-2 application (middle), and after washout (bottom). Calibration bars: 50 μV, 0.5 s. (**B–C**) Quantification of SWR properties across conditions. (**B**) Inter-event interval (IEI). (**C**) Sharp wave amplitude. No significant effects of WIN55,212-2 were observed. (**D**) Peri-event time histograms of multiunit activity (MUA) aligned to SWR peak under control (left), WIN55,212-2 (middle), and washout (right) conditions. (**E–G**) Quantification of neuronal activity parameters. (**E**) Baseline firing rate (MUA-Base). (**F**) SWR-associated firing rate (MUA-SWR). (**G**) MUA delay relative to SWR peak (MUA-Delay). No significant effects of WIN55,212-2 were detected for any parameter. Statistical analysis was performed using LMM (Control vs WIN55,212-2). Washout data are shown for completeness but were not included in statistical comparisons.

3.4. Effects of Vehicle (DMSO) on SWRs and Neuronal Activity

Because CBD was dissolved in DMSO, we first assessed whether the vehicle itself affects spontaneous network activity. Application of DMSO did not significantly alter any of the examined SWR or MUA parameters (Figures 6 and 7). No significant main effects of condition were observed for IEI, cluster probability, amplitude, ripple frequency, ripple power, MUA-Base, MUA-SWR, or MUA-Delay (all $p > 0.25$), and no condition × region interactions were detected. In contrast, significant dorsoventral differences persisted for several parameters, including IEI, cluster probability, ripple

 doi:10.20944/preprints202604.1018.v1

power, and MUA-SWR (all $p < 0.05$), confirming that vehicle application does not interfere with the intrinsic organization of hippocampal network activity.

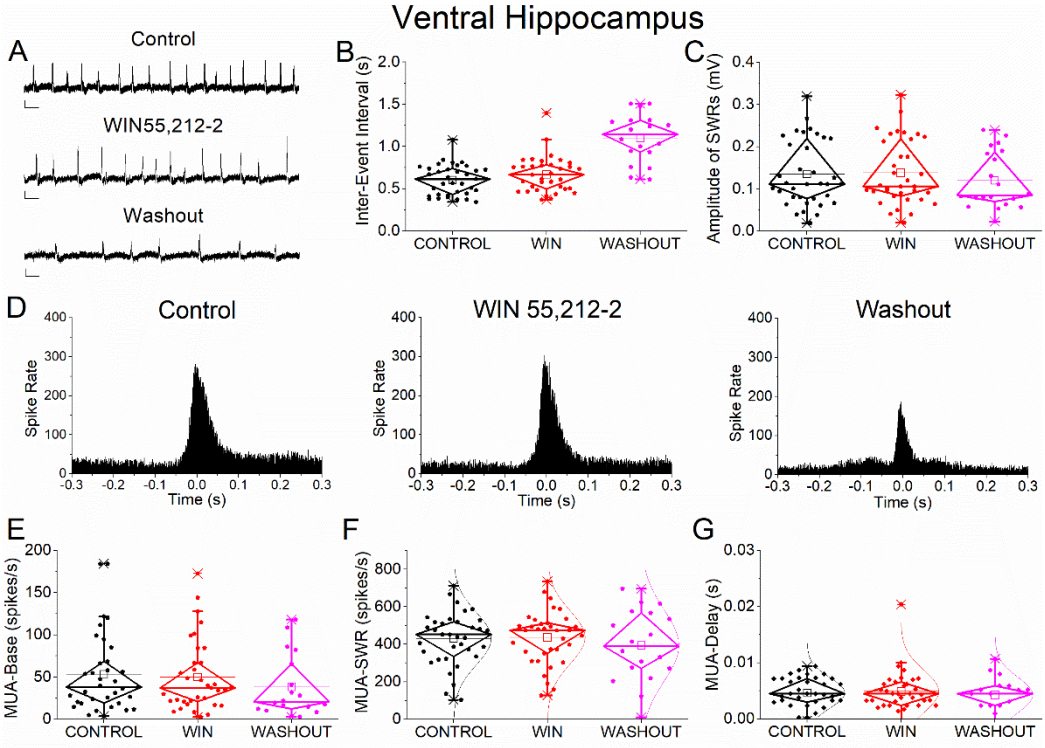

Figure 5. Effects of the cannabinoid receptor agonist WIN55,212-2 on SWRs and MUA in ventral hippocampus. (**A**) Representative extracellular recordings from CA1 stratum pyramidale under control conditions (top), during WIN55,212-2 application (middle), and after washout (bottom). Calibration bars: 50 μV, 0.5 s. (**B–C**) Quantification of SWR properties across conditions. (**B**) Inter-event interval (IEI). (**C**) Sharp wave amplitude. No significant effects of WIN55,212-2 were observed. (**D**) Peri-event time histograms of multiunit activity (MUA) aligned to SWR peak under control (left), WIN55,212-2 (middle), and washout (right) conditions. (**E–G**) Quantification of MUA parameters. (**E**) Baseline firing rate (MUA-Base). (**F**) SWR-associated firing rate (MUA-SWR). (**G**) MUA delay relative to SWR peak (MUA-Delay). No significant effects of WIN55,212-2 were detected for any parameter. Statistical analysis was performed using LMM (Control vs WIN55,212-2). Washout data were not included in statistical comparisons.

3.5. Effects of Cannabidiol (CBD) on Hippocampal Sharp Wave–Ripples

We next examined whether the CBD influences hippocampal network oscillations associated with SWRs. CBD did not significantly affect SWR dynamics or neuronal activity when compared with vehicle (DMSO). LMM analysis revealed no significant effect of condition on IEI, cluster probability, amplitude, ripple frequency, ripple power, MUA-Base, MUA-SWR, or MUA-Delay (all $p > 0.08$) (Figures 6 and 7). No significant condition × region interactions were observed for any parameter, indicating that CBD did not differentially influence dorsal and ventral hippocampal activity (Figures 6 and 7). These findings indicate that CBD does not modulate spontaneous SWRs or associated neuronal firing under the present experimental conditions.

3.6. Effects of TPN-Q on SWR and Neuronal Activity

To assess the contribution of GIRK-dependent conductances to hippocampal network dynamics, TPN-Q was applied prior to cannabinoid receptor activation. TPN-Q did not significantly affect IEI, SWR amplitude, ripple frequency, MUA-Base, MUA-SWR, or MUA-Delay (all $p > 0.5$) (Figures 8 and 9), and no condition × region interactions were observed. In contrast, TPN-Q significantly increased ripple power ($p = 0.003$), indicating a selective effect on the high-frequency oscillatory component of

 doi:10.20944/preprints202604.1018.v1

SWRs. These results suggest that GIRK channel activity contributes to the modulation of ripple oscillations without significantly affecting SWR occurrence or neuronal recruitment.

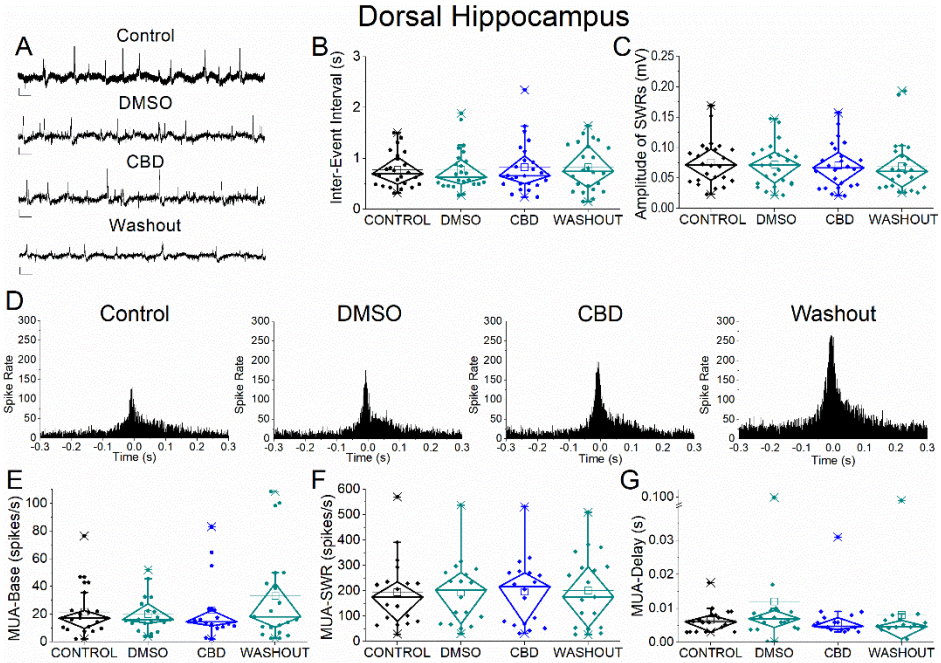

Figure 6. Effects of vehicle (DMSO) and cannabidiol (CBD) on SWRs and MUA in dorsal hippocampus. (**A**) Representative extracellular recordings from CA1 stratum pyramidale under control conditions (top), during application of DMSO (second trace), CBD (third trace), and after washout (bottom). Calibration bars: 50 μV, 0.5 s. (**B–C**) Quantification of SWR properties across conditions. (**B**) Inter-event interval (IEI). (**C**) Sharp wave amplitude. Neither DMSO nor CBD produced significant effects. (**D**) Peri-event time histograms of multiunit activity (MUA) aligned to SWR peak under control, DMSO, CBD, and washout conditions. (**E–G**) Quantification of neuronal activity parameters. (**E**) Baseline firing rate (MUA-Base). (**F**) SWR-associated firing rate (MUA-SWR). (**G**) MUA delay relative to SWR peak (MUA-Delay). No significant effects of DMSO or CBD were detected for any parameter. Statistical analysis was performed using LMM (Control vs DMSO and Control vs CBD); washout data were not included in statistical comparisons.

3.7. Effects of WIN on SWR and Neuronal Activity in the Presence of TPN-Q

To determine whether GIRK channel blockade modifies the effects of cannabinoid receptor activation, WIN 55,212-2 was applied in the presence of TPN-Q. Under these conditions, WIN did not significantly affect any of the examined properties of spontaneous SWRs or associated neuronal activity. LMM analysis revealed no significant effect of condition on inter-event interval (IEI), sharp wave amplitude, ripple frequency, or ripple power (all $p > 0.5$) (Figures 8 and 9). Similarly, WIN did not alter baseline multiunit activity (MUA-Base), SWR-associated neuronal firing (MUA-SWR), or the temporal delay of neuronal firing relative to SWR peaks (MUA-Delay) (all $p > 0.4$) (Figures 8 and 9). No significant condition × region interactions were observed for any parameter, indicating that GIRK channel blockade does not unmask or modify the effects of WIN in either dorsal or ventral hippocampus. In contrast, significant main effects of hippocampal segment persisted for several parameters, including SWR amplitude, ripple power, and MUA-SWR (all $p < 0.05$), confirming robust dorsoventral differences in network activity that were not influenced by the combined application of TPN-Q and WIN.

Preprints.org (www.preprints.org) | NOT PEER-REVIEWED | Posted: 15 April 2026 doi:10.20944/preprints202604.1018.v1

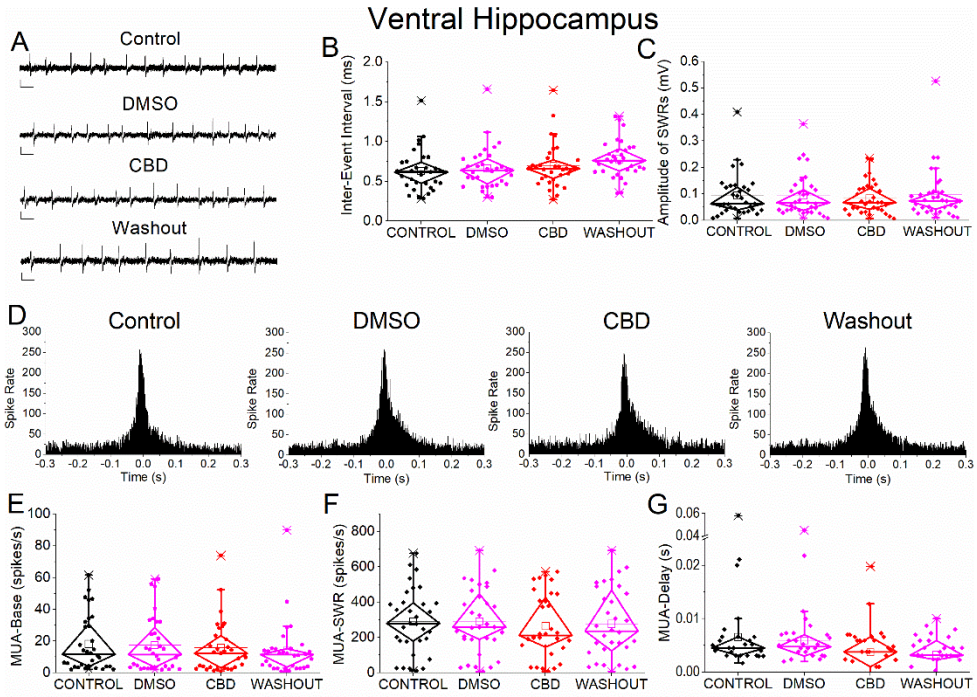

Figure 7. Effects of vehicle (DMSO) and cannabidiol (CBD) on SWRs and associated neuronal activity in ventral hippocampus. (**A**) Representative extracellular recordings from CA1 stratum pyramidale under control conditions (top), during application of DMSO (second trace), CBD (third trace), and after washout (bottom). Calibration bars: 50 µV, 0.5 s. (**B–C**) Quantification of SWR properties across conditions. (**B**) Inter-event interval (IEI). (**C**) Sharp wave amplitude. Neither DMSO nor CBD produced significant effects. (**D**) Peri-event time histograms of multiunit activity (MUA) aligned to SWR peak under control, DMSO, CBD, and washout conditions. (**E–G**) Quantification of neuronal activity parameters. (**E**) Baseline firing rate (MUA-Base). (**F**) SWR-associated firing rate (MUA-SWR). (**G**) MUA delay relative to SWR peak (MUA-Delay). No significant effects of DMSO or CBD were detected for any parameter. Statistical analysis was performed using LMM (Control vs DMSO and Control vs CBD). Washout data were not included in statistical comparisons.

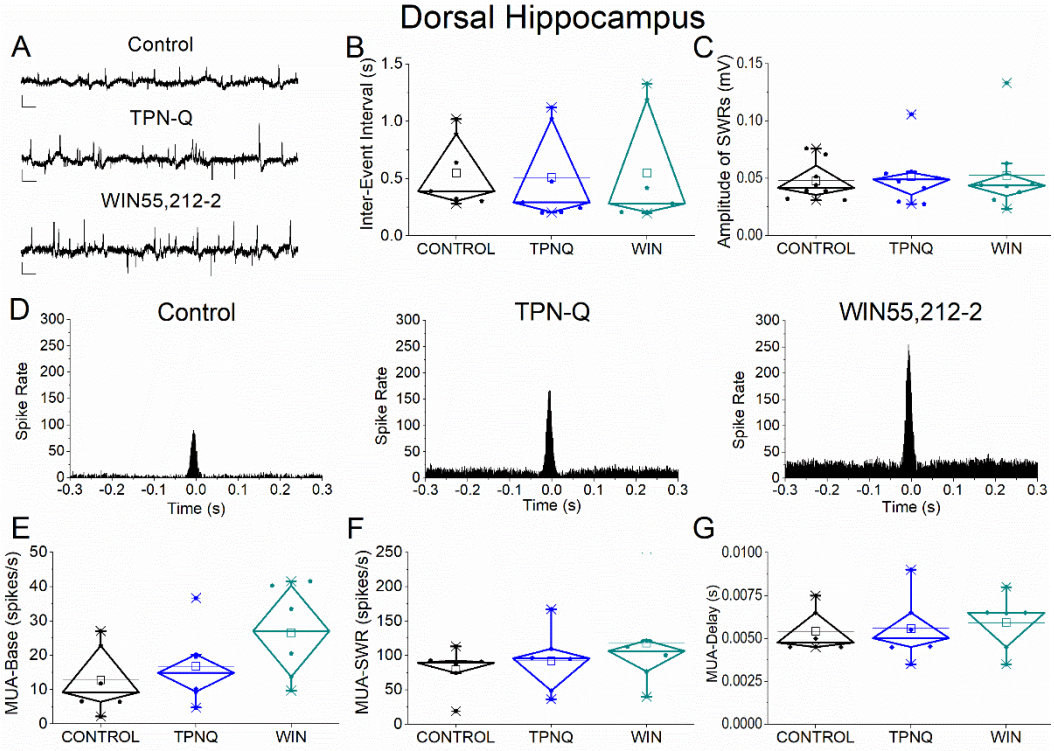

 doi:10.20944/preprints202604.1018.v1

Figure 8. Effects of GIRK channel blockade with TPN-Q and subsequent application of WIN55,212-2 on SWRs and associated neuronal activity in dorsal hippocampus. (**A**) Representative extracellular recordings from CA1 stratum pyramidale under control conditions (top), during TPN-Q application (middle), and after subsequent application of WIN55,212-2 (bottom). Calibration bars: 50 μV, 0.5 s. (**B–C**) Quantification of SWR properties across conditions. (**B**) Inter-event interval (IEI). (**C**) Sharp wave amplitude. TPN-Q produced no significant effects on SWR properties, and subsequent application of WIN55,212-2 did not alter these parameters. (**D**) Peri-event time histograms of MUA aligned to SWR peak under control (left), TPN-Q (middle), and WIN55,212-2 (right) conditions. (**E–G**) Quantification of neuronal activity parameters. (**E**) Baseline firing rate (MUA-Base). (**F**) SWR-associated firing rate (MUA-SWR). (**G**) MUA delay relative to SWR peak (MUA-Delay). TPN-Q produced only minor, non-significant changes, and no additional effects were observed following WIN55,212-2 application. Statistical analysis was performed using LMM (Control vs TPN-Q and TPN-Q vs WIN55,212-2).

3.8. CB1 Receptor Expression is Comparable Between Dorsal and Ventral Hippocampus

Notably, the lack of detectable effects of CB1 receptor agonists on SWR activity, despite comparable receptor expression, further suggests that CB1-mediated signaling does not play a major role in the regulation of spontaneous SWRs under these conditions. To this end, we performed Western blot analysis to compare CB1 receptor levels in dorsal and ventral hippocampus. Quantitative analysis revealed no significant difference in CB1 receptor expression between dorsal and ventral hippocampal samples (paired t-test, $t = -0.31$, $p = 0.772$; Figure 10). These findings indicate that the functional differences in SWR dynamics along the dorsoventral axis are unlikely to arise from differences in the overall abundance of CB1 receptors. Instead, they may reflect region-specific variations in receptor localization, circuit organization, or downstream signaling mechanisms.

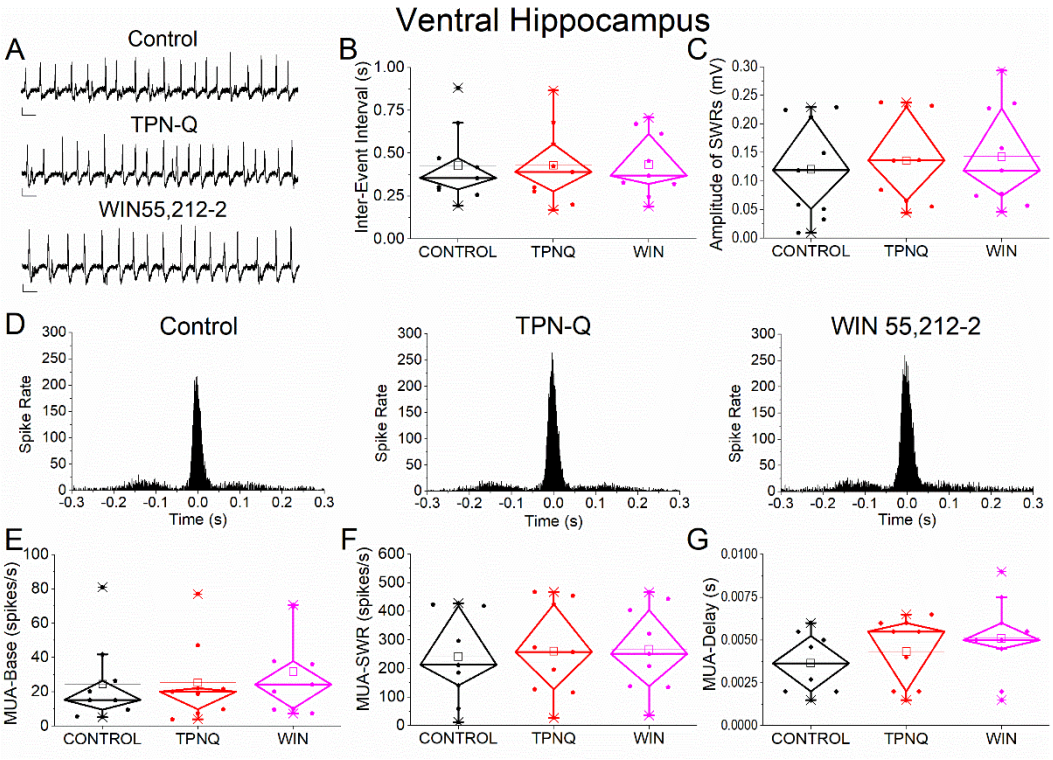

Figure 9. Effects of GIRK channel blockade with TPN-Q and subsequent application of WIN55,212-2 on SWRs and MUA in ventral hippocampus. (**A**) Representative extracellular recordings from CA1 stratum pyramidale under control conditions (top), during TPN-Q application (middle), and after subsequent application of WIN55,212-2 (bottom). Calibration bars: 50 μV, 0.5 s. (**B–C**) Quantification of SWR properties across conditions. (**B**) Inter-event interval (IEI). (**C**) Sharp wave amplitude. TPN-Q produced no significant effects on SWR properties, and subsequent application of WIN55,212-2 did not alter these parameters. (**D**) Peri-event time histograms of MUA aligned to SWR peak under control (left), TPN-Q (middle), and WIN55,212-2 (right)

 doi:10.20944/preprints202604.1018.v1

conditions. (**E–G**) Quantification of MUA parameters. (**E**) Baseline firing rate (MUA-Base). (**F**) SWR-associated firing rate (MUA-SWR). (**G**) MUA delay relative to SWR peak (MUA-Delay). TPN-Q produced only limited, non-significant effects, and no additional effects were observed following WIN55,212-2 application. Statistical analysis was performed using LMM (Control vs TPN-Q and TPN-Q vs WIN55,212-2).

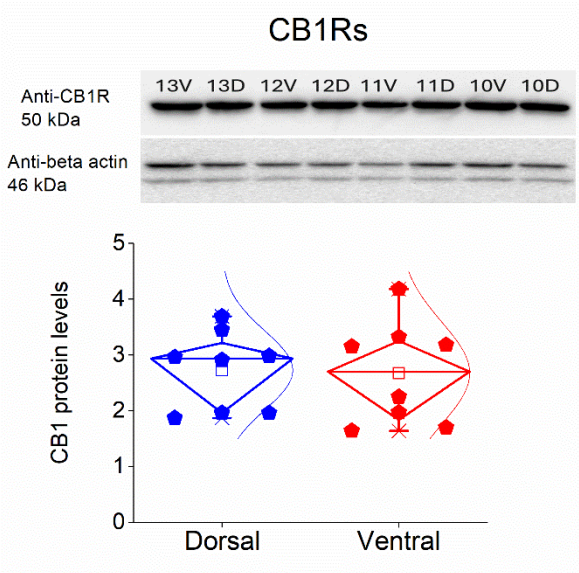

Figure 10. Comparable CB1 receptor expression in CA3 dorsal and ventral hippocampal region. Representative Western blot showing CB1 receptor immunoreactivity (~50 kDa) in dorsal (D) and ventral (V) hippocampal samples, with β-actin (~46 kDa) used as loading control (top). Lane labels indicate individual samples from dorsal and ventral hippocampus. Quantification of CB1 protein levels (normalized to β-actin) revealed no significant difference between dorsal and ventral hippocampus. Data are presented as individual samples from corresponding rats, with distributions illustrated using box plots.

4. Discussion

The present study demonstrates that spontaneous SWR activity in hippocampal slices exhibits pronounced dorsoventral differences but is largely resistant to acute pharmacological manipulation of the endocannabinoid system. Across all tested conditions, including selective CB1 receptor activation (ACEA), non-selective cannabinoid receptor activation (WIN 55,212-2), CBD, and GIRK channel blockade, no significant changes were observed in SWR occurrence, waveform properties, or associated neuronal firing. In contrast, robust and consistent differences between dorsal and ventral hippocampus were evident across multiple parameters, including SWR rate, amplitude, ripple characteristics, and MUA recruitment. These findings indicate that, under baseline in vitro conditions, SWR-generating circuits operate largely independently of acute cannabinoid modulation, while their intrinsic dorsoventral organization remains a dominant determinant of network dynamics.

Previous studies have reported that cannabinoid receptor activation suppresses hippocampal oscillations and disrupts SWRs, reducing their incidence, ripple power, and associated neuronal recruitment (Robbe et al., 2006; Maier et al., 2012; Sun et al., 2012; Kim et al., 2024). In contrast, the present study did not detect significant effects of CB1 receptor activation or CBD on SWR properties. This apparent discrepancy may reflect, at least in part, differences in analytical approaches and pharmacological specificity. In several previous reports, the observed cannabinoid-induced changes appear relatively modest in magnitude and may depend on statistical sensitivity, as paired comparisons can enhance detection of small within-slice effects compared to more conservative models such as the linear mixed approach used here, which explicitly accounts for between-slice variability. In addition, studies employing endogenous cannabinoids such as anandamide may

 doi:10.20944/preprints202604.1018.v1

involve activation of multiple targets beyond CB1 receptors, including TRPV1 channels (Sun-2012), leading to more complex and variable network effects. Thus, previously reported alterations in SWR dynamics may arise from a combination of CB1-dependent and non-canonical mechanisms, as well as from differences in analytical sensitivity. Overall, the present findings suggest that intrinsic SWR-generating circuits are relatively resistant to acute cannabinoid modulation.

A central finding of this study is the persistence of strong dorsoventral differences in SWR dynamics across all experimental conditions. Ventral hippocampus exhibited higher SWR rates, larger amplitudes, and stronger neuronal recruitment, consistent with previous in vitro work [23–26]. These differences likely reflect intrinsic variations in circuit organization, synaptic dynamics, and excitation–inhibition balance along the hippocampal axis. Importantly, these regional characteristics were not modified by cannabinoid receptor activation or GIRK channel blockade, suggesting that the mechanisms underlying dorsoventral specialization operate independently of acute endocannabinoid signaling. This reinforces the view that SWR dynamics are primarily governed by structural and synaptic properties of local circuits, rather than by fast neuromodulatory control.

Blockade of GIRK channels with TPN-Q produced only limited effects on SWR dynamics, with the exception of a selective modulation of ripple power. This finding suggests that GIRK-dependent conductances may contribute to the fine-tuning of high-frequency oscillatory synchronization, without playing a major role in SWR generation or neuronal recruitment. Notably, in a previous study (Trompoukis et al., 2020), GIRK blockade increased SWR rate in the dorsal hippocampus and enhanced the probability of clustered events, indicating a role in the temporal organization of network activity. The absence of such effects in the present dataset may reflect differences in analytical approach, as well as the lack of cluster analysis, which was previously identified as a sensitive parameter for GIRK-dependent modulation. Interestingly, GIRK blockade did not reveal any latent sensitivity of SWRs to cannabinoid receptor activation, as combined application of TPN-Q and WIN also failed to alter SWR or MUA parameters. This indicates that the lack of cannabinoid effects observed in this study is not simply due to masking by GIRK-mediated mechanisms.

Western blot analysis showed comparable levels of CB1 receptor expression in dorsal and ventral hippocampal CA3, indicating that the observed dorsoventral differences in SWR dynamics are not attributable to differences in receptor abundance. Instead, they are more likely related to regional differences in circuit architecture, synaptic organization, or downstream signaling pathways. Notably, similar dissociation between receptor expression and functional output has been reported in CA1 hippocampal circuits, where CB1 receptor levels were comparable between dorsal and ventral regions despite pronounced differences in network excitability and short-term neuronal dynamics (Tsotsokou et al., 2025), suggesting that dorsoventral functional specialization of cannabinoid signaling is primarily determined by circuit-level and intracellular mechanisms rather than receptor density per se.

Taken together, these findings suggest that CB1 receptor expression alone is not sufficient to predict functional modulation of network activity, particularly in the context of intrinsically generated oscillations such as SWRs. SWRs are widely implicated in memory consolidation, replay, and hippocampal—cortical communication [1,34–36]. Disruption of SWRs by cannabinoids has been proposed as a mechanism underlying cannabinoid-induced memory impairment [12,14]. The present findings suggest that such effects may depend critically on network state and circuit context, and may not arise from direct suppression of intrinsic SWR-generating mechanisms. Instead, cannabinoid-induced alterations in memory may involve modulation of input pathways, network coordination, or large-scale brain dynamics, rather than local SWR generation per se. This distinction is important for understanding how cannabinoids influence hippocampal function in vivo and for interpreting their cognitive and behavioral effects.

5. Conclusions

In summary, our results demonstrate that spontaneous SWRs in hippocampal slices are robust to acute cannabinoid modulation, despite clear dorsoventral differences in network dynamics and

 doi:10.20944/preprints202604.1018.v1

comparable CB1 receptor expression. These findings highlight the resilience of intrinsic hippocampal circuits and suggest that cannabinoid effects on memory-related activity are likely mediated through mechanisms beyond local SWR generation.

Author Contributions: Conceptualization, C.P.; investigation, A.M., P.G., A.E., A-I.T., E-D.M., G.T., I-M. S.; formal analysis, A.M., P.G., A.E., A-I.T., E-D.M., G.T., I-M. S., C.P.; resources, C.P.; writing-original draft preparation, C.P.; writing-review and editing, A.M., C.P.; supervision, C.P.; project administration, C.P.; funding acquisition, C.P. all authors have read and agreed to the published version of the manuscript.

Funding: The research project was supported by the Empeirikeion Foundation (#10). A.M. is a recipient of a postgraduate fellowship from the Hellenic Foundation for Research and Innovation (HFRI). G.T. was financially supported by the "Polembros Shipping Limited", as a recipient of Ph.D. fellowships.

Institutional Review Board Statement: The animal study protocol was approved by the Research Ethics Committee of the University of Patras and the Directorate of Veterinary Services of the Achaia Prefecture of Western Greece Region (reg. number: 5661/37, 18 January 2021). The treatment of animals and all experimental procedures used in this study were conducted in accordance with the European Communities Council Directive Guidelines for the care and use of Laboratory animals (2010/63/EU—European Commission).

Informed Consent Statement: Not applicable.

Data Availability Statement: The minimal dataset supporting the conclusions of this study, including all variables used for statistical analysis, is available from the corresponding author upon reasonable request.

Acknowledgments: The authors would like to thank Dr. Leonidas Leontiadis and Mr. George Trompoukis for their valuable technical assistance in this study. The authors also gratefully acknowledge Dr. Maria Chalampalaki (Faculty of Pharmacy, National and Kapodistrian University of Athens) for the generous provision of cannabidiol, which was essential for the completion of this work.

Conflicts of Interest: The authors declare no conflict of interest.

Abbreviations

The following abbreviations are used in this manuscript:

ACEA	N-(2-Chloroethyl)-5Z,8Z,11Z,14Z-eicosatetraenamide
ACSF	Artificial cerebrospinal fluid
CBD	Cannabidiol
CB1	Cannabinoid receptor type 1
E/I	Excitation/Inhibition balance
FFT	Fast Fourier Transform
GIRK	G-protein-gated inwardly rectifying potassium channels
IEI	Inter-event interval
LFP	Local field potential
LMM	Linear mixed-effects model
MUA	Multiunit activity
MUA-Base	Baseline multiunit activity
MUA-Delay	Delay of multiunit activity relative to SWR peak
MUA-SWR	SWR-associated multiunit activity
SWR	Sharp wave–ripple
TPN-Q	Tertiapin-Q
WIN 55,212-2	[(3R)-2,3-dihydro-5-methyl-3-(4-morpholinylmethyl)pyrrolo[1,2,3-de]-1,4-benzoxazin-6-yl]-1-naphthalenylmethanone

References

1. Buzsaki, G. Hippocampal sharp wave-ripple: A cognitive biomarker for episodic memory and planning. *Hippocampus* **2015**, *25*, 1073-1188, doi:10.1002/hipo.22488.

 doi:10.20944/preprints202604.1018.v1

2. Jadhav, S.P.; Kemere, C.; German, P.W.; Frank, L.M. Awake hippocampal sharp-wave ripples support spatial memory. *Science* **2012**, *336*, 1454-1458, doi:10.1126/science.1217230.
3. Girardeau, G.; Zugaro, M. Hippocampal ripples and memory consolidation. *Current opinion in neurobiology* **2011**, *21*, 452-459, doi:10.1016/j.conb.2011.02.005.
4. Mechoulam, R.; Parker, L.A. The endocannabinoid system and the brain. *Annu Rev Psychol* **2013**, *64*, 21-47, doi:10.1146/annurev-psych-113011-143739.
5. Lu, H.C.; Mackie, K. An Introduction to the Endogenous Cannabinoid System. *Biological psychiatry* **2016**, *79*, 516-525, doi:10.1016/j.biopsych.2015.07.028.
6. Katona, I.; Freund, T.F. Multiple functions of endocannabinoid signaling in the brain. *Annual review of neuroscience* **2012**, *35*, 529-558, doi:10.1146/annurev-neuro-062111-150420.
7. Kawamura, Y.; Fukaya, M.; Maejima, T.; Yoshida, T.; Miura, E.; Watanabe, M.; Ohno-Shosaku, T.; Kano, M. The CB1 cannabinoid receptor is the major cannabinoid receptor at excitatory presynaptic sites in the hippocampus and cerebellum. *The Journal of neuroscience : the official journal of the Society for Neuroscience* **2006**, *26*, 2991-3001, doi:10.1523/jneurosci.4872-05.2006.
8. Howlett, A.C.; Barth, F.; Bonner, T.I.; Cabral, G.; Casellas, P.; Devane, W.A.; Felder, C.C.; Herkenham, M.; Mackie, K.; Martin, B.R.; et al. International Union of Pharmacology. XXVII. Classification of cannabinoid receptors. *Pharmacological reviews* **2002**, *54*, 161-202, doi:10.1124/pr.54.2.161.
9. Kano, M.; Ohno-Shosaku, T.; Hashimotodani, Y.; Uchigashima, M.; Watanabe, M. Endocannabinoid-mediated control of synaptic transmission. *Physiological reviews* **2009**, *89*, 309-380, doi:10.1152/physrev.00019.2008.
10. Wilson, R.I.; Nicoll, R.A. Endogenous cannabinoids mediate retrograde signalling at hippocampal synapses. *Nature* **2001**, *410*, 588-592, doi:10.1038/35069076.
11. Kreitzer, A.C.; Regehr, W.G. Cerebellar depolarization-induced suppression of inhibition is mediated by endogenous cannabinoids. *The Journal of neuroscience : the official journal of the Society for Neuroscience* **2001**, *21*, Rc174, doi:10.1523/JNEUROSCI.21-20-j0005.2001.
12. Robbe, D.; Montgomery, S.M.; Thome, A.; Rueda-Orozco, P.E.; McNaughton, B.L.; Buzsaki, G. Cannabinoids reveal importance of spike timing coordination in hippocampal function. *Nature neuroscience* **2006**, *9*, 1526-1533, doi:nn1801 [pii] 10.1038/nn1801.
13. Holderith, N.; Németh, B.; Papp, O.I.; Veres, J.M.; Nagy, G.A.; Hájos, N. Cannabinoids attenuate hippocampal γ oscillations by suppressing excitatory synaptic input onto CA3 pyramidal neurons and fast spiking basket cells. *The Journal of physiology* **2011**, *589*, 4921-4934, doi:10.1113/jphysiol.2011.216259.
14. Maier, N.; Morris, G.; Schuchmann, S.; Korotkova, T.; Ponomarenko, A.; Bohm, C.; Wozny, C.; Schmitz, D. Cannabinoids disrupt hippocampal sharp wave-ripples via inhibition of glutamate release. *Hippocampus* **2012**, *22*, 1350-1362, doi:10.1002/hipo.20971.
15. Sun, Y.; Norimoto, H.; Pu, X.P.; Matsuki, N.; Ikegaya, Y. Cannabinoid receptor activation disrupts the internal structure of hippocampal sharp wave-ripple complexes. *Journal of pharmacological sciences* **2012**, *118*, 288-294.
16. Laprairie, R.B.; Bagher, A.M.; Kelly, M.E.; Denovan-Wright, E.M. Cannabidiol is a negative allosteric modulator of the cannabinoid CB1 receptor. *British journal of pharmacology* **2015**, *172*, 4790-4805, doi:10.1111/bph.13250.
17. Priestley, R.; Glass, M.; Kendall, D. Functional Selectivity at Cannabinoid Receptors. *Adv Pharmacol* **2017**, *80*, 207-221, doi:10.1016/bs.apha.2017.03.005.
18. Pretzsch, C.M.; Freyberg, J.; Voinescu, B.; Lythgoe, D.; Horder, J.; Mendez, M.A.; Wichers, R.; Ajram, L.; Ivin, G.; Heasman, M.; et al. Effects of cannabidiol on brain excitation and inhibition systems; a randomised placebo-controlled single dose trial during magnetic resonance spectroscopy in adults with and without autism spectrum disorder. *Neuropsychopharmacology : official publication of the American College of Neuropsychopharmacology* **2019**, *44*, 1398-1405, doi:10.1038/s41386-019-0333-8.
19. Fanselow, M.S.; Dong, H.W. Are the dorsal and ventral hippocampus functionally distinct structures? *Neuron* **2010**, *65*, 7-19, doi:10.1016/j.neuron.2009.11.031.
20. Bannerman, D.M.; Sprengel, R.; Sanderson, D.J.; McHugh, S.B.; Rawlins, J.N.; Monyer, H.; Seeburg, P.H. Hippocampal synaptic plasticity, spatial memory and anxiety. *Nat Rev Neurosci* **2014**, *15*, 181-192.

 doi:10.20944/preprints202604.1018.v1

21. Strange, B.A.; Witter, M.P.; Lein, E.S.; Moser, E.I. Functional organization of the hippocampal longitudinal axis. *Nat Rev Neurosci* **2014**, *15*, 655-669, doi:10.1038/nrn3785.
22. Papatheodoropoulos, C. Electrophysiological evidence for long-axis intrinsic diversification of the hippocampus. *Frontiers in Bioscience (Landmark Ed.)*. **2018**, *23*, 109-145., doi:10.2741/4584.
23. Kouvaros, S.; Papatheodoropoulos, C. Prominent differences in sharp waves, ripples and complex spike bursts between the dorsal and the ventral rat hippocampus. *Neuroscience* **2017**, *352*, 131-143, doi:10.1016/j.neuroscience.2017.03.050.
24. Trompoukis, G.; Rigas, P.; Leontiadis, L.J.; Papatheodoropoulos, C. I(h), GIRK, and KCNQ/Kv7 channels differently modulate sharp wave—ripples in the dorsal and ventral hippocampus. *Molecular and cellular neurosciences* **2020**, *107*, 103531, doi:10.1016/j.mcn.2020.103531.
25. Leontiadis, L.J.; Trompoukis, G.; Tsotsokou, G.; Miliou, A.; Felemegkas, P.; Papatheodoropoulos, C. Rescue of sharp wave-ripples and prevention of network hyperexcitability in the ventral but not the dorsal hippocampus of a rat model of fragile X syndrome. *Frontiers in cellular neuroscience* **2023**, *17*, doi:10.3389/fncel.2023.1296235.
26. Kandilakis, C.L.; Papatheodoropoulos, C. Serotonin Modulation of Dorsoventral Hippocampus in Physiology and Schizophrenia. **2025**, *26*, 7253.
27. Trompoukis, G.; Rigas, P.; Leontiadis, L.J.; Papatheodoropoulos, C. Ih, GIRK, and KCNQ/Kv7 channels differently modulate sharp wave—ripples in the dorsal and ventral hippocampus. *Molecular and cellular neurosciences* **2020**, 103531, doi:10.1016/j.mcn.2020.103531.
28. Trompoukis, G.; Leontiadis, L.J.; Rigas, P.; Papatheodoropoulos, C. Scaling of Network Excitability and Inhibition may Contribute to the Septotemporal Differentiation of Sharp Waves-Ripples in Rat Hippocampus In Vitro. *Neuroscience* **2021**, *458*, 11-30, doi:10.1016/j.neuroscience.2020.12.033.
29. Patel, J.; Schomburg, E.W.; Berényi, A.; Fujisawa, S.; Buzsáki, G. Local generation and propagation of ripples along the septotemporal axis of the hippocampus. *The Journal of neuroscience : the official journal of the Society for Neuroscience* **2013**, *33*, 17029-17041, doi:10.1523/JNEUROSCI.2036-13.2013.
30. Sosa, M.; Joo, H.R.; Frank, L.M. Dorsal and Ventral Hippocampal Sharp-Wave Ripples Activate Distinct Nucleus Accumbens Networks. *Neuron* **2019**, S0896-6273(0819)31008-31006, doi:10.1016/j.neuron.2019.11.022.
31. Swanson, L.W.; Wyss, J.M.; Cowan, W.M. An autoradiographic study of the organization of intrahippocampal association pathways in the rat. *The Journal of comparative neurology* **1978**, *181*, 681-715, doi:10.1002/cne.901810402.
32. Ishizuka, N.; Weber, J.; Amaral, D.G. Organization of intrahippocampal projections originating from CA3 pyramidal cells in the rat. *The Journal of comparative neurology* **1990**, *295*, 580-623.
33. Sullivan, D.; Csicsvari, J.; Mizuseki, K.; Montgomery, S.; Diba, K.; Buzsáki, G. Relationships between hippocampal sharp waves, ripples, and fast gamma oscillation: influence of dentate and entorhinal cortical activity. *The Journal of neuroscience : the official journal of the Society for Neuroscience* **2011**, *31*, 8605-8616, doi:10.1523/JNEUROSCI.0294-11.2011.
34. Maingret, N.; Girardeau, G.; Todorova, R.; Goutierre, M.; Zugaro, M. Hippocampo-cortical coupling mediates memory consolidation during sleep. *Nature neuroscience* **2016**, *19*, 959-964, doi:10.1038/nn.4304.
35. Yu, J.Y.; Frank, L.M. Hippocampal-cortical interaction in decision making. *Neurobiology of learning and memory* **2015**, *117*, 34-41, doi:10.1016/j.nlm.2014.02.002.
36. Colgin, L.L. Rhythms of the hippocampal network. *Nat Rev Neurosci* **2016**, *17*, 239-249, doi:10.1038/nrn.2016.21.